Modern Chemistry
2020; 8(2): 23-32
http://www.sciencepublishinggroup.com/j/mc
doi: 10.11648/j.mc.20200802.12
ISSN: 2329-1818 (Print); ISSN: 2329-180X (Online)

Batch Equilibrium and Kinetic Studies of Anionic and Cationic Dyes Adsorption onto Al−Pillared Clay from a Local Cameroonian Clay Materials in Aqueous Medium

Massai Harouna[1], Constant Tcheka[1, *], Narcisse Dobe[2]

[1]Faculty of Science, University of Ngaoundere, Ngaoundere, Cameroon
[2]Faculty of Science, University of Maroua, Maroua, Cameroon

Email address:

harounamassai@yahoo.fr (M. Harouna), ctcheka@yaho.com (C. Tcheka), dobe.narcisse@yahoo.fr (N. Dobe)
[*]Corresponding author

To cite this article:

Massaï Harouna, Constant Tcheka, Narcisse Dobe. Batch Equilibrium and Kinetic Studies of Anionic and Cationic Dyes Adsorption onto Al−Pillared Clay from a Local Cameroonian Clay Materials in Aqueous Medium. *Modern Chemistry*. Vol. 8, No. 2, 2020, pp. 23-32.
doi: 10.11648/j.mc.20200802.12

Received: July 29, 2020; **Accepted**: August 19, 2020; **Published**: August 27, 2020

Abstract: The present work report removal of acid red 14 (AR14) and basic violet 3 (BV3) as anionic and cationic dyes, respectively, by adsorption process in batch mode from aqueous solution onto natural and modified forms of a local Cameroonian clay. The efficiency of these adsorbents materials (purified natural clay, P−Clay, sodium−clay, Na−Clay, and aluminium−pillared, Al−PILC) to remove dyes from aqueous medium was examined at different initial concentrations, pH, and ionic strengths. At the optimal contact time of 20 minutes, the maximum adsorbed dye amount on various adsorbents was obtained at pH 9 and pH 3 for AR14 and BV3 dyes, respectively. Adsorption process of both dyes on purified or modified clay was pH depend and the dyes molecules sorption over the clay surface occurs by electrostatic interactions. Ionic strength influenced significantly AR14 and BV3 dyes adsorption. Homo-ionization and pillaring clay increased its adsorption capacity. Kinetic studies showed that adsorption follows a pseudo−second−order model, and rate constants were evaluated. Non-linear fit of adsorption isotherm, q_e *vs* C_e, were *S*−class for adsorption of both dye onto AL−PILC, indicating the heterogeneity of the adsorbent surface which leaded to a multilayer adsorption with interactions between dye molecules. Langmuir and Freundlich models were the best fits to the experimental data with the maximum adsorption capacities of AL−PILC for AR14 and BV3 dyes of 1.4 mg g^{-1} and 3.0 mg g^{-1}, respectively. Lower adsorption capacities calculated from Langmuir isotherm model than the experimental values indicated adsorption mechanism occurs by multilayer formation on the adsorbent surface.

Keywords: Pillared Clay, Acid Red 14, Basic Violet 3, Kinetic Studies, Adsorption Isotherms

1. Introduction

Water is an essential resource for live on the planet and human development. The textile industry is one of the anthropogenic activities that most consume water and pollute water bodies [1]. Dyes are widely used in papermaking and printing, food activities, cosmetic, and clinical industries, but especially in textile industries due to their chemical stability and ease of synthesis and variety of colors [2]. However, these dyes become the pollution source when released into environment. During various steps of dyeing process, high or less significant amounts of dyes are lost due to a lack of affinity with the surfaces to be dyed or colored and are found in the waste. At the end of the coloring process, an estimated amount of used dye of 10 to 15% is found in wastewater [2, 3]. However, these organic compounds are carcinogenic and refractory to the treatment processes usually implemented and are resistant to biodegradation [4]. The development of new methods and optimization of existing processes, which must be efficient and inexpensive, are the principal goal of several previous works [2−6]. Several methods of dyes removal from contaminated water have been developed in research laboratories, e.g. electrocoagulation, biological treatment, advanced oxidation process, ion exchange, adsorption, filtration, electrodialysis, membrane separation, magnetic

separation [5, 7−9]. Among these methods, adsorption was the most used for its flexibility, easily and simplicity to implement and yielded purified water with high quality [10]. In addition, residual solid from adsorption process can be recycled or confined in construction materials. Although activated carbon is the most promising absorbent material, its use remain limited because its fabrication is relatively expensive and the regeneration of the adsorbent for several steps may cause difficulties [11]. Hence this cost problem has led to a search for cheap and efficient alternate materials including clay materials. Several papers reported utilization of biomass materials based adsorbents, agricultural wastes, activated silica, biopolymer (chitosan, alginate) based composites, zeolite, fly ash, metal oxides and clays [5, 12, 13]. Clay is abundant in the subsoil, it present high adsorption capacity and ion exchange properties and, have been used many time as adsorbent for organic and inorganic pollutants removal in waste water [14]. Adsorption efficiency of clays increases when modified with pillaring agents or organically modified [5, 11, 15]. In the present work, a sample of purified local Cameroonian clay was homo-ionized with sodium, then pillared by aluminium and its efficiency as adsorbent was tested for removal of anionic (basic violet 3) and cationic (acid red 14) dyes from aqueous solution. Valorization of this clay as low cost adsorbent and natural resource for water treatment is also expected. The effects of certain parameters such as contact time, adsorbent dose, pH, ionic strength and initial concentration of the dye solution were studied. Furthermore, the kinetic and isotherm models were determined, and adsorption mechanism of both dyes on the surface of pillared clay was also proposed.

2. Materials and Methods

2.1. Reagents

The samples of both dyes in powder solid forms were purchased from SIGMA−ALDRICH Corporation. Their structures and essential chemical characteristics are presented in table 1. Stock solutions of 1 g/L of AR14 and BV3 dyes were prepared by dissolving 1 g of each dye in 1000 mL of distilled water and the derived solutions with desired concentrations were obtained by dilution operations. NaOH and HCl diluted solutions were used to adjust the pH values.

Table 1. *Structures and chemical characteristics of AR14 and BV3 dyes.*

Structures/Properties	Carmoisine	Crystal Violet
Structure	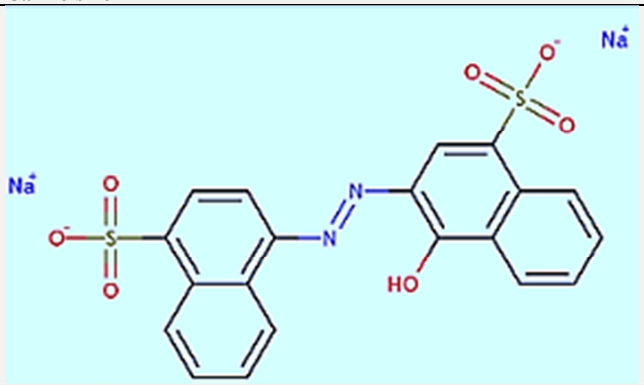	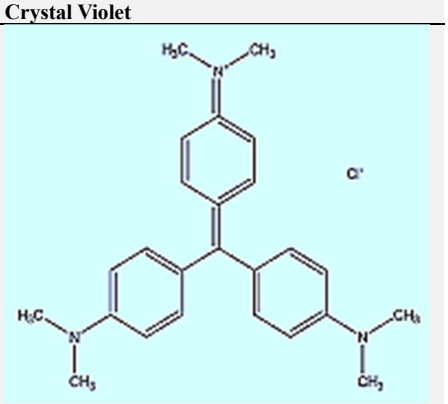
Nature	anionic	cationic
C.I. name	Acid red 14	Basic violet 3
C.I. number	14720	42555
Chemical formula	$C_{20}H_{12}N_2Na_2O_7S_2$	$C_{25}H_{30}N_3Cl$
Molecular weight	502.428±0.029	407.979±0.025
λ_{max}	516 nm	600 nm

2.2. Preparation of Pillared Clay

The natural clay used in this work was obtained from Boboyo's deposit in the Kaele Sub Division, Far-North Region of Cameroon. This clay material has been characterized and described in previous works [16, 17]. Its physico-chemical properties reported in previous work are given in table 2.

Table 2. *Summary properties of raw clay [14, 15].*

Parameters	Values
Moisture content (%)	22.39
pH	8.53
Rising index (%)	95.98
Density	1.39
CEC (meq/100 g)	74
S_{BET} (m^2/g)	111
Micropore volume (cm^3/g)	0.0009
Mesopore volume (cm^3/g)	0.145
Mineralogical composition (%)	Illite: 62.2; Kaolinite: 27.0; Quartz: 10.4

The starting clay, Na-saturated sample was prepared by treatment of purified natural clay with 1 N sodium chloride solution, with subsequent washing by centrifugation and to move excess chloride. The obtained solid was dried in oven at 80°C for 24 h. Aluminium-pillared clay was prepared following the procedure described by Yamanaka and Brindley, and Khedher and co-workers [18, 19]. The pillaring solution

(OH/Al = 2) was prepared by titrating 0.1 N NaOH aqueous solution with aqueous 0.1 N $AlCl_3.6H_2O$ aqueous solution. NaOH solution (300 mL, 30 mmol) was added dropwise to $AlCl_3$ solution (150 mL, 15 mmol) at a constant rate of 1ml/min. Then the pillaring solution was agitated for 2 h at 60°C and then aged overnight at room temperature. After aging, the resulting solution (350 mL, 15 mmol of Al) was reacted with 3 g of aqueous suspension of Na-clay (Al/clay ratio = 5 mmol/g). The slurry was agitated at temperature of 60 ºC for 2 h, then washed with distillated water and centrifuged till the absence of chloride (test $AgNO_3$ 0.01 N) and oven-dried at 80 ºC for 20 h and calcined at 400°C for 3 h. the resulting material was named Al-PILC.

2.3. Batch Adsorption Experiments

Adsorption experiments were conducted in batch mode using 200 mL conical flasks containing a total volume of 20 mL of the reaction solution. Reaction mixture (adsorbent + dye solution) was agitated at constant speed of 300 rpm using a magnetic stirrer (SBS-MR-1600/1T Model) for the required time. The effect of some operating parameters such as, contact time (5−120 min), absorbent dosage (0.01−0.20 g), initial solution pH (2−12) and dye concentration (0.5−20 ppm), on the dyes adsorption were studied. After each adsorption experiment completed, the solid phase was separated from the liquid phase by centrifugation of the aqueous solution at 5000 rpm for 5 min. The initial and residual dye concentrations in aqueous phase were measured using a UV/Vis spectrophotometer (SOCOMAM-PRIM spectrophotometer model) at maximal wavelength values of 516 nm and 600 nm for AR14 and BV3, respectively. The amount of dye adsorbed per gram of absorbent, q_e (mg g^{-1}) were calculated using the equation (1):

$$q_e = \frac{(C_0 - C_e) \times V}{m} \quad (1)$$

where C_0 and C_e (ppm) are initial and residual dye concentrations at initial and equilibrium time, respectively, V (L) is the volume of the reaction solution, and m (g) is the mass of adsorbent.

For kinetic experiments, predetermined optimum adsorbent mass of 0.01 g was contacted with 20 mL of dye solution, initial concentration of 14 ppm. The amount of dye adsorbed at time t (min), q_t (mg g^{-1}), was calculated by equation (2):

$$q_t = \frac{(C_0 - C_t) \times V}{m} \quad (2)$$

where C_t (min) is the dye concentration at specific time t.

3. Results and Discussion

3.1. Adsorption Experiments

3.1.1. Effect of Contact Time

Evaluation of the effect of contact time is essential because it provides fundamental information on how fast the adsorption process reaches equilibrium. From the results presented in Figure 1, it was observed the fast dye adsorption at initial stage, which became gradually slower as equilibrium was approached. Pillared clay (Al-PILC) had highest adsorption capacity, followed by Na-Clay and P-Clay. The time required to reach equilibrium was found to be 20 minutes for adsorption of both dyes on the three clay materials. The rapid adsorption process at the initial stage could be attributed to the easily accessible active sites on the adsorbent surfaces and the slow adsorption rate in later stage was apparently due to slower diffusion of dye molecules into the interior of the adsorbents [20]. Indeed, numerous and vacant active surface sites of adsorbent were available in the early stages of the adsorption, while as the contact time increased, the number of vacant sites decreased, thereby slowing down the adsorption process. Similarly, the increase of the initial dye concentration led to higher loading rates of the adsorbate molecule, which was attributed to the enhanced driving force of the concentration gradient to the vacant sites of adsorbent [17, 21, 22]. Therefore, the adsorption time was fixed to 20 min in all adsorption experiments to make sure that the adsorption reached equilibrium.

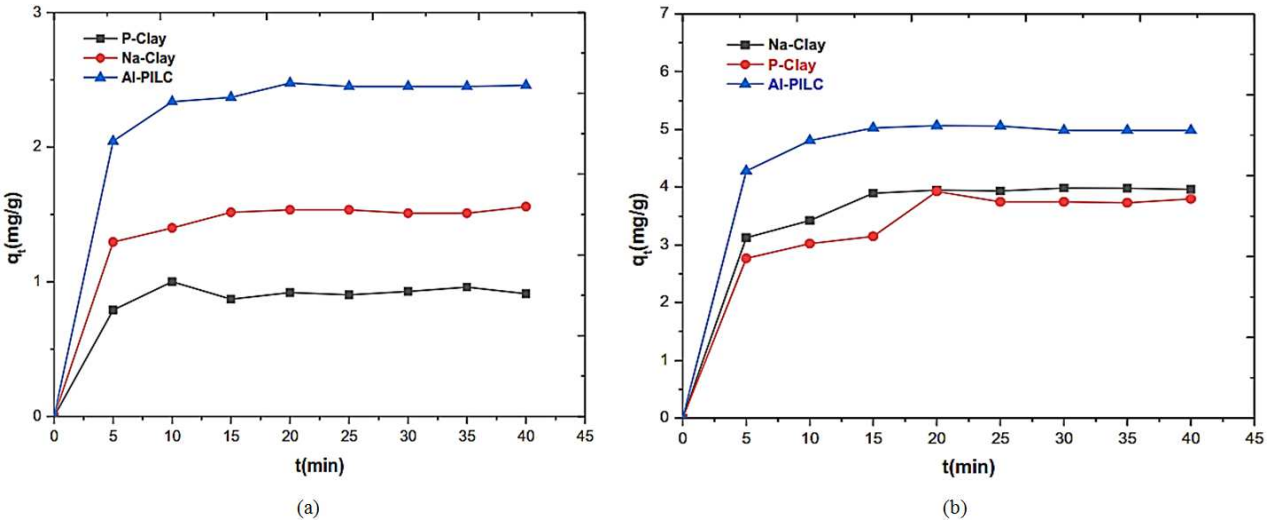

Figure 1. *Effect of contact time on adsorbed quantity of AR14 (a) and BV3 (b) on the three adsorbents. Conditions: initial dye concentration 14 ppm, 25±°C, 300 rpm.*

3.1.2. Effect of Adsorbent Dose

P−Clay, Na−Clay and Al−PILC quantity influence over AR14 and BV3 adsorption is presented in Figure 2. It can be seen that as the adsorbent amount increases, adsorption capacity decreases. In fact, until adsorbent amount remain weak in solution, dye molecules can easily reached adsorption sites. The decrease in adsorbed amount at higher dosage is due to a decrease in the number of occupied sites per unit mass [23−25]. This may also be ascribed to the total adsorption surface area available to dye molecules resulting from overlapping or aggregation of adsorption sites [7]. For further experiments, 0.01 g was used as adsorbent mass.

3.1.3. Effect of Solution pH

The influence of pH over dye adsorption onto purified and modified clays was studied while the initial dye concentration, contact time and adsorbent amount were fixed at 14 ppm, 20 min and 0.01 g, respectively. As presented in figure 3, the variation of dye adsorption on the three adsorbent materials over a pH range of 2.0–12.0 revealed that the adsorption of AR14 dye increased with an increase in pH of the solution from 3.0 to 9.0, while for BV3 dye its adsorption variation decreased from pH 3.0 to 9.0 and then remained almost constant. It can be also observed that maximum adsorbed amount on various adsorbents was obtained at pH 9 and pH 3 for AR14 and BV3, respectively. This observation indicates that adsorption of both dyes was pH dependent. When the pH of the reaction solution decreased, the number of positively charged sites on the clay surface increased, and the number of negatively charged sites decreased. The negatively charged sites on the adsorbent surface favored the adsorption of cationic dye due to electrostatic interaction. The lower adsorption at acid pH was due to the presence of excess H+ competing with the AR14 dye for adsorption sites. Lower sorption of the anionic dye at alkaline pH could be attributed to the abundance of OH^- ions which will compete with the BV3 anions for the same sorption sites [15, 26, 27]. Further adsorption experiments were conducted at initial solutions pH of 9.0 for AR14 and 3.0 for BV3.

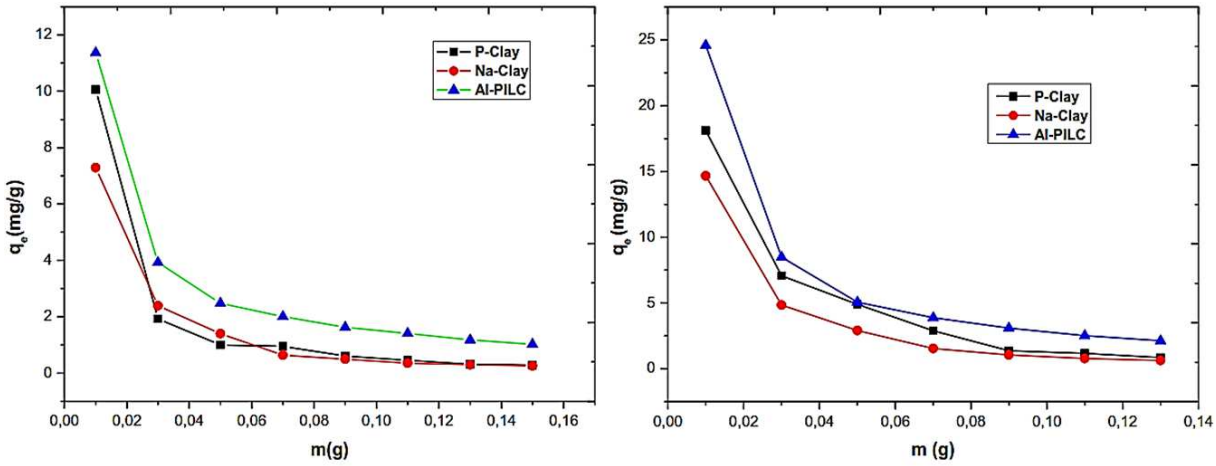

Figure 2. *Effect of adsorbent dose on AR14 (a) adsorption and BV3 (b) adsorption. Conditions: initial dye concentration 14 ppm, contact time 20 min, 25±2°C.*

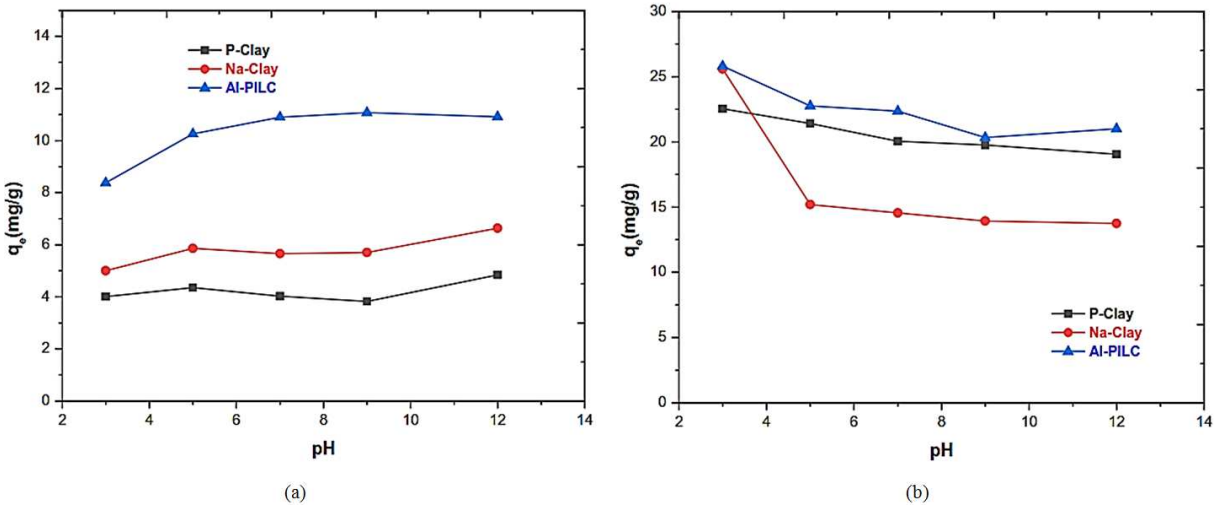

Figure 3. *Effect of pH solution on AR14 (a) and BV3 (b) dyes adsorption.*

3.1.4. Effect of Initial Dye Concentration

The effect of the initial dye concentrations over the adsorption capacity of AR14 and BV3 dyes on the three adsorbents are shown in Figure 4. It can be observed that the adsorption amount of both dyes onto all adsorbents increase continuously with the initial AR14 and BV3 dye concentrations up to 14 ppm at the given adsorption conditions: T (25°C), pH (9.0) for AR14 and pH (3.0) for BV3, contact time (20 min), adsorbent mass (0.01 g). AR14 and BV3 adsorption on all the clay samples did not show a plateau suggesting that there was no formation of monolayer on the surface of the adsorbents [28].

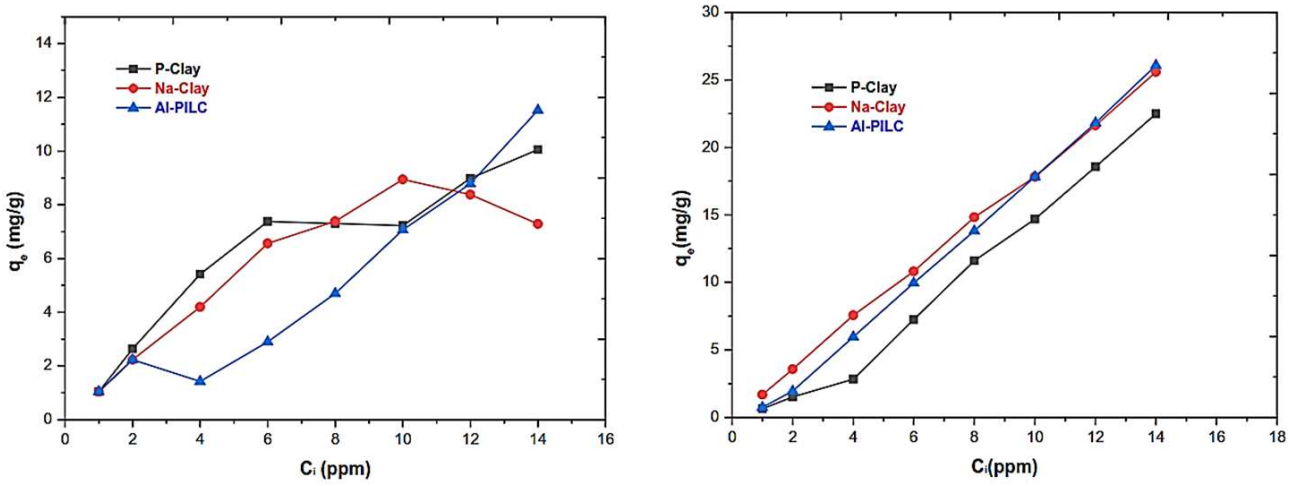

Figure 4. *Effect of initial dye concentrations on AR14 (a) and BV3 (b) adsorption amount.*

3.1.5. Effect of Ionic Strength

Electrostatic and non-electrostatic interactions between dye molecules and adsorbent surface can be influenced by ionic strength of the solution [7]. In order to explore the effect of ionic strength of the solution on AR14 and BV3 adsorption, NaCl solutions with different concentrations values ranging from 100 to 500 ppm were prepared and 20 mL was added to the dye solutions. Experimental study of variation of adsorption capacity with NaCl concentration was carried out at initial dyes concentration of 14 ppm at 25 ± 2°C. The ionic strength effect is presented in Figure 5. As can be seen, the adsorbed dye quantity increased as the concentration of NaCl increased up to 200 ppm for both AR14 and BV3. After this concentration, a slight decrease in adsorbed amounts is observed for AR14 adsorption, while it remained almost constant for BV3. In the first hand, this observation could be attributed to the NaCl addition, which does not affect the interaction between AR14 molecules and active sites on adsorbent [7, 29]. The slight decrease in adsorption for the salt concentration over 100 ppm (Figure 5 (a)) can be attributed to competitive adsorption between AR14 ions and increasing sodium ions with increasing of NaCl concentrations on the negatively charged clay at pH 9 [7]. In the other hand, BV3 dye adsorption capacity remained constant for the salt concentration over 200 ppm (Figure 5 (b)), this could be explained by the slight influence of ionic strength on its adsorption.

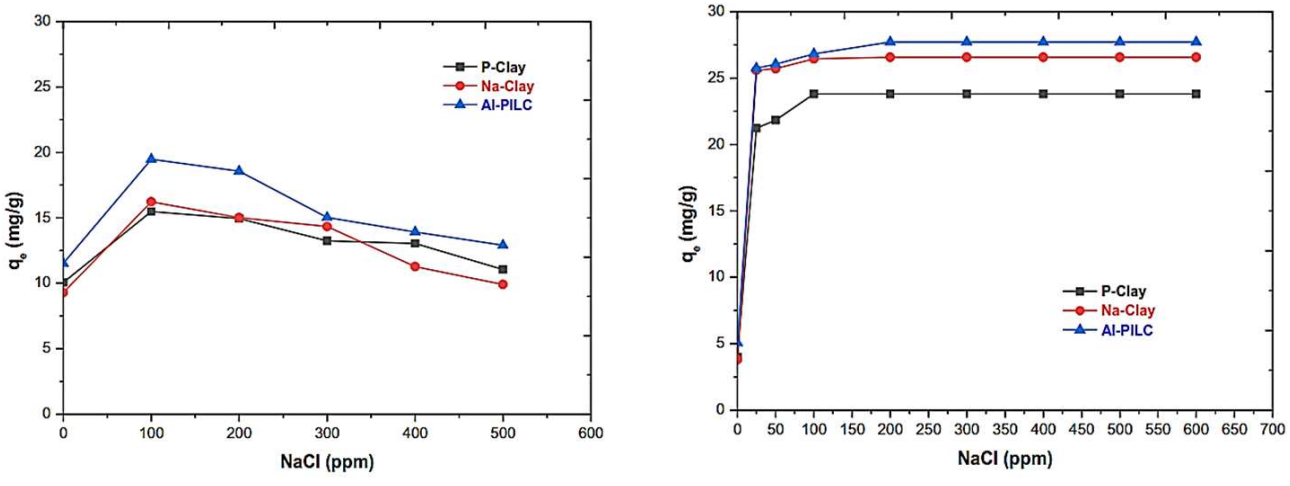

Figure 5. *Effect of ionic strength on AR14 (a) (pH 9) and BV3 (b) (pH 3) adsorption.*

3.2. Adsorption Kinetics

Adsorption kinetic studies are conducted in adsorption process in order to examine the mechanisms controlling. Several kinetic models are available in the literature to describe and better understand the behavior and kinetics of adsorbents. In this work, four kinetic models were used to represent the AR14 and BV3 dyes adsorption on the three adsorbents, namely: Pseudo-first-order, Pseudo-second-order, Intra-particle diffusion and Elovich models. The best fit of the experimental data was established based on the value of the coefficient of determination R^2. The linearized form of the pseudo-first-order model deduced from the model established by Lagergren [30] was given by equation (3).

$$ln(q_e - q_t) = ln(q_e) - \frac{k_1.t}{2.303} \quad (3)$$

where q_e and q_t represent the amount of dye adsorbed (mg g^{-1}) at equilibrium and at specific time t (min), respectively. k_1 is the Lagergren 1st order rate constant (min^{-1}). The plot of $ln(q_e - q_t)$ as a function of t was used to determine the parameters of the pseudo-first-order model (Tables 3 and 4).

The linear equation of the pseudo−second−order kinetic model was given by equation (4) [31] (Ho and McKay 19 99):

$$\frac{t}{q_t} = \frac{1}{k_2 q_e^2} + \frac{1}{q_e} t \quad (4)$$

where k_2 is the pseudo-second-order rate constant (g mg^{-1} min^{-1}). The plot of t/q_t versus t (Figure 6) was used to determine the parameters of the pseudo−second−order kinetic model.

The linear form of Elovich model [32] was represented by equation (5).

$$q_t = \frac{1}{\beta} ln(\alpha\beta) + \frac{1}{\beta} ln(t) \quad (5)$$

where α is the adsorption rate constant and β is the adsorption constant related to the extent of surface coverage and activation energy for chemisorption. These constants were calculated from the straight line obtained by plotting q_t versus ln(t) (Tables 3 and 4).

To evaluate the contribution of dyes diffusion through the adsorbent pores, the rate constant for intra-particle diffusion k_{id} (mg g^{-1} $m^{-1/2}$) and the thickness of the boundary layer C_i (mg g^{-1}) were also determined using Weber and Morris model [33] (equation (6)).

$$q_t = k_{id}.t^{1/2} + C_i \quad (6)$$

The values of k_{id}, C_i and R^2 obtained by plotting q_t versus $t^{1/2}$ are represented in Tables 3 and 4. The experimentally determined amounts of dyes (AR14 or BV3), $q_{e,exp}$, and the calculated values, i.e., $q_{e,cal}$ derived from the simulation of adsorption kinetics (pseudo-first-, and pseudo-second-order models) are shown in tables 3 and 4. The pseudo-second-order R^2 values (0.995; 0.994, and 0.999 for AR14 adsorption, 0.991; 0.980 and 0.998 for BV3 adsorption) on various adsorbents were higher than the other models values and closer to 1. However, $q_{e,cal}$ values determined for the pseudo-second-order model were mainly close to the $q_{e,exp}$ values. Thus the simulation results suggest that the adsorption of AR14 and BV3 dyes fit the pseudo-second-order kinetic model quit well, and this kinetic model could be applied to describe adsorption mechanism of AR14 and BV3 dyes adsorption onto clay materials. Figure 7 shows the amounts of adsorbed dye, q_e, function of $t^{1/2}$ for different adsorbent materials. As can be observed, plots are linear over the range of time and the lower values of k_{id} (Tables 3 and 4) which indicate that one of sorption, chemisorption involved in the AR14 and BV3 adsorption and slow diffusion through the adsorbent pores. Based on these, it can be concluded that diffusion in not the adsorption limiting step. [32].

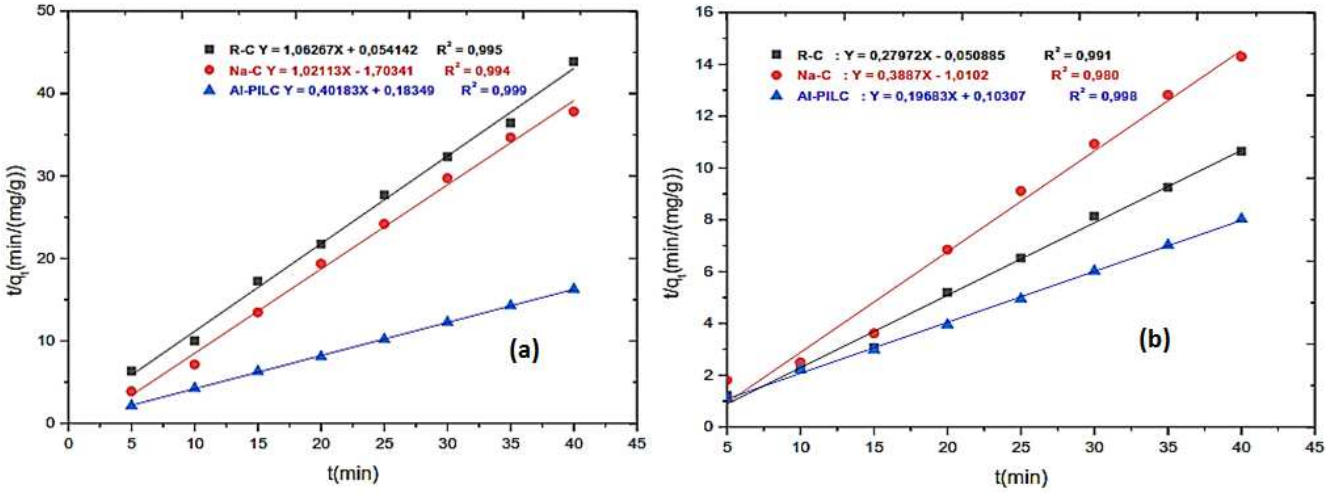

Figure 6. *Plot of linearized form of pseudo-second-order equation for AR14 (a) and BV3 (b) adsorption onto the three clay materials (V = 20 mL, pH 9 for AR14 and pH 3 for BV3, m_{Clay} = 0.01 g, T = 25 ± 2°C).*

Table 3. *Kinetic parameters for the adsorption of AR14 dye onto P−Clay, Na−Clay and Al−PILC (V = 20 mL, pH 9, m_{Clay} = 0.01 g, T = 25 ± 2°C).*

Adsorbent	Pseudo-first-order				Pseudo-second-order			Elovich equation			Intra-particle diffusion		
	$q_{e,exp*}$ (mg g^{-1})	k_1 (min^{-1})	$q_{e,cal*}$ (mg g^{-1})	R^2	k_2 (g/min.g)	$q_{e,cal}$ (mg g^{-1})	R^2	β	α	R^2	C_i (mg g^{-1})	k_{id*} (mg g^{-1} min$^{-1/2}$)	R^2
P-Clay	0.960	0.05	0.967	0.556	2.08	0.941	0.995	22.98	2.83×10^{6}	0.112	0.82	0.01	0.047
Na-Clay	1.558	0.01	0.970	0.516	0.61	0.979	0.994	5.73	2×10^{3}	0.640	1.51	0.08	0.611
Al-PILC	2.459	0.07	0.934	0.889	0.87	2.489	0.999	14.51	6.3×10^{12}	0.686	2.26	0.03	0.673

Note:*e,exp = eqpilibrium, experimental; *e,cal =eqilibrium, calculated; *id = intra-particle diffusion

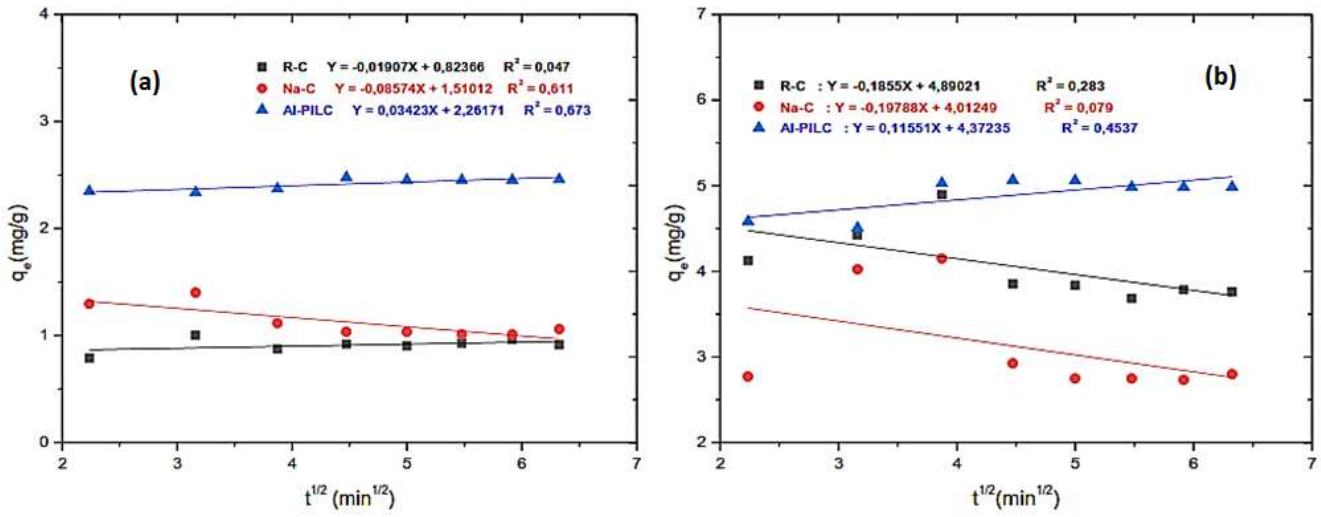

Figure 7. *Plot of linearized form of intra-particle diffusion equation for AR14 (a) and BV3 (b) adsorption onto the three clay materials (V = 20 mL, pH 9 for AR14 and pH 3 for BV3, m_{Clay} = 0.01 g, T = 25 ± 2°C).*

Table 4. *Kinetic parameters for the adsorption of BV3 dye onto P−Clay, Na-Clay and Al−PILC (V = 20 mL, pH 3, m_{Clay} = 0.01 g, T = 25 ± 2°C).*

Adsorbent	Pseudo-first-order				Pseudo-second-order			Elovich equation			Intra-particle diffusion		
	$q_{e,exp}$ (mg^{-1}g)	k_1 (min^{-1})	$q_{e,cal}$ (mg/g)	R^2	k_2 (g/min.g)	$q_{e,cal}$ (mg g^{-1})	R^2	β	α	R^2	C_i (mg g^{-1})	K_{id} (mg g^{-1} min$^{-1/2}$)	R^2
P-Clay	3.986	0.01	1.020	0.492	0.16	3.575	0.991	2.99	1.16×10^{5}	0.198	4.12	0.18	0.283
Na-Clay	3.798	0.03	1.034	0.072	0.14	2.573	0.980	3.10	9.54×10^{4}	0.003	4.01	0.19	0.079
Al-PILC	4.836	0.05	0.948	0.067	0.37	5.098	0.998	4.06	5.77×10^{6}	0.538	4.67	0.11	0.454

Note:*e,exp = eqpilibrium, experimental; *e,cal =eqilibrium, calculated; *id = intra-particle diffusion

3.3. Adsorption Isotherms

The adsorption isotherms indicate how the adsorbate molecules (AR14 or BV3 dye) were distributed between the liquid and the solid phases when the adsorption process reaches an equilibrium state. Figure 8 gives the adsorption isotherms at temperature of 25 ± 2°C for AR14 and BV3 dyes on AL−PILC. It can be observed the AR14 or BV3 dye adsorbed amount increased slowly with increasing the initial concentration. According to the classification of Giles and co-corkers [35], both dyes showed a *S*-class isotherm. This type of isotherm is characteristic of multilayer adsorption due to the strong adsorbate-adsorbate interaction [34].

In order to understand the adsorption phenomenon, the experimental isotherm data of AR14 and BV3 dyes adsorption onto the three Clay adsorbents were analyzed by fitting them to four theoretical isotherm models, Langmuir, [37], Freundlich, [38], Temkin, [39], and Dubinin-Radushkevich (DR) [40, 41].

The Langmuir model is presented by the following equation:

$$q_e = \frac{q_m k_L C_e}{1+k_L C_e} \quad (7)$$

where q_e (mg g^{-1}), q_m (mg g^{-1}), C_e (mg L^{-1}) and K_L (L mg^{-1}) are adsorbed amount of dye at equilibrium, Langmuir maximum adsorption capacity, dye concentration at equilibrium and Langmuir constant, respectively.

The Freundlich model, is given by equation (8).

$$q_e = K_F C_e^{1/n_F} \quad (8)$$

where k_F [mg/g(L/mg)$^{1/n}$], is the Freundlich constant and indicator of the adsorption capacity of the adsorbent while n_F indicates favorability of the adsorption process (adsorption intensity) or surface heterogeneity. n_F value between 1 and 10 represents favorable adsorption.

The Temkin isotherm model is expressed by following equation:

$$q_e = \frac{RT}{b_T} ln(k_T C_e) \quad (9)$$

where k_T (L mg^{-1}) is the equilibrium binding constant corresponding to the maximum binding energy, b_T (J mol^{-1}) is related to the adsorption heat, R is the universal gas constant (8.314 J k^{-1} mol^{-1}) and T is the temperature (K).

The Dubinin-Radushkevich (D-R) isotherm assumes a Gaussian-type distribution for the characteristic curve and the model can be described by equation (10).

$$q_e = q_D e^{-k_{ad}\varepsilon^2} \quad (10)$$

where q_D (mol g^{-1}), is the theoretical isotherm saturation capacity, B_D (mol^2 kJ^{-2}), gives the mean sorption free energy E (kJ/mol) per molecule of adsorbed at the moment of its transfer to the solid surface from the bulk solution [37] and can be computed using equation (11).

$$E = \frac{1}{\sqrt{2B_D}} \quad (11)$$

The D-R isotherm model considers that adsorbent size is comparable to the micropore size and the adsorption equilibrium relation for a given adsorbate-adsorbent combination can be expressed independently of temperature by using the adsorption potential (ε) (equation (12).

$$\varepsilon = RT\ ln\left(1 + \frac{1}{C_e}\right) \quad (12)$$

The nonlinear plots of the studied isotherm models relate to equations (7) – (10) applicate on the data of AR14 and BV3 dyes adsorption on AL−PILC adsorbent are displayed in Figure 8. The fit quality of each isotherm model was evaluated through the determination coefficient R2.

The isotherm parameters of models were presented in Tables 5 and 6. By comparing the values of linear constant regression, R^2, the Langmuir and Freundlich isotherm models have the highest values practically equal to 1, followed by the Temkin, and Dubinin-Radushkevich models for various adsorbents, which indicates that Langmuir model was the best fit to the experimental data. The maximum adsorption capacities of Al-PILC for AR14 and BV3 dyes were found to be 1.4 mg g^{-1} and 3.0 mg g^{-1}, respectively. The relatively low adsorption capacity of AL-PILC than experimental values (11.2 mg g^{-1} for AR14 dye and 24.95 mg g^{-1} for BV3 dye adsorption), can be explained by the heterogeneity of the adsorbent surface which would lead to a multilayer adsorption with interactions between adsorbate molecules (AR14 or BV3 dye molecules) [8].

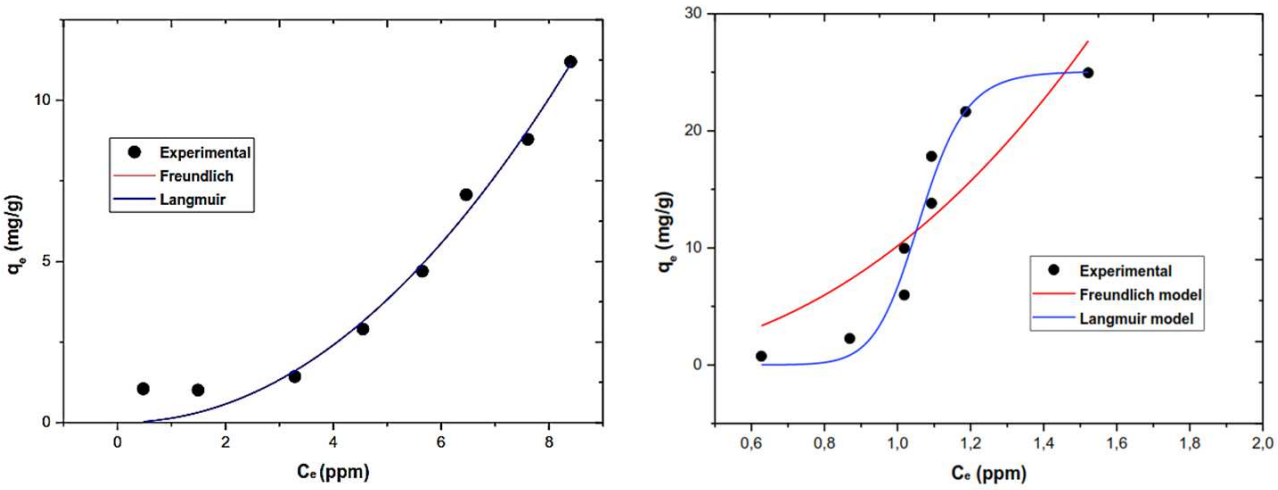

(a) (b)

Figure 8. *Adsorption isotherms AR14 dye (a) and BV3 dye (b) by AL-PILC. Conditions: contact time 20 min, 25 ±2° C, V = 20 mL, m = 0.01 g.*

The n_F values (equal to 1 for adsorption of both dyes onto all adsorbent materials), indicate that adsorption of AR14 and BV3 on various clays adsorbents is a favorable and linear, processing with high and intensity, indicating the heterogeneity in dye molecules and clay surface system, and involve constant adsorbent-adsorbate affinity [42]. The free energy values, E, obtained from D-R isotherm model were (1291 kJ mol^{-1} for AR14 adsorption, and 845.1 and 1000 kJ mol^{-1} for BV3) onto P−Clay, Na−Clay and Al−PILC, respectively. These values of E > 80 kJ mol^{-1}, indicate that adsorption of both dyes on various clay materials in this study take place as chemisorption [43].

Table 5. *Isotherm parameters for the adsorption of AR14 dye onto P−Clay, Na−Clay, and Al−PILC.*

Adsorbent	Freundlich						Temkin			DR			
	k_{L*}×10^{-7}	q_{m*}(mg g)	R^2	k_{F*}	n_F	R^2	k_T	b	R^2	E (kJ/mol)	B_{D*}×10^{-7}	q_m(mg/g)	R^2
R-C	–	–	1	1.99	1	1	1.96	3.84	0,92	1291	3	7.96	0.85
Na-C	–	–	1	1	1	1	0.99	3.70	0,93	1291	3	7.57	0.89
Al-PILC	1.4	1.4	1	1.99	1	1	1.79	4.16	0,91	1291	3	7.45	0.85

Note:*L = Langmuir; *m = maximal; *T = Temkin; *D = Dubinin

Table 6. *Isotherm parameters for the adsorption of BV3 dye onto P−Clay, Na−Clay and Al−PILC.*

Adsorbents	Langmuir			Freundlich			Temkin			DR			
	$K_L \times 10^{-8}$	q_m (mg/g)	R^2	k_F	n_F	R^2	k_T	b	R^2	E (kJ mol^{-1})	$B_D \times 10^{-7}$	q_m (mg/g)	R^2
P−Clay	3.6	1.11	1	0.39	1	1	1.86	1.17	0.85	1000	5	3.17	0.89
Na−Clay	6.6	2.6	1	1.99	1	1	0.95	8.47	0.88	845.1	7	15.54	0.79
Al−PILC	6.6	3.0	1	1.99	1	1	1.61	6.71	0.83	1000	5	21.03	0.92

Note:*L = Langmuir; *m = maximal; *T = Temkin; *D = Dubinin

4. Conclusion

A local purified natural clay and its modified form (Na−Clay and Al−PILC), were tested as adsorbent for Acid Red 14 and Basic Violet 3 dyes removal from aqueous solutions. The study of effect of contact time over adsorption of both dyes revealed a rapid process with the equilibrium time of 20 minutes. The influence of solution pH showed that the maximum amount of AR14 dye adsorbed was observed at alkaline pH (pH 9), while the adsorption capacity for BV3 was lower in alkaline medium and the maximum was obtained at pH 3. From this observation, the adsorption process of AR14 and BV3 dyes on various adsorbents could preceded by electrostatic interaction between dye charges and those on the clay surface. Application of kinetic models to analyze the adsorption mechanism of AR14 and BV3 dyes on various adsorbents showed that the pseudo-second-order model with R^2 values higher and closer to 1 than the other models, and $q_{e, cal}$ values determined for the pseudo-second-order model were mainly close to the $q_{e, exp}$ values indicating that the pseudo-second-order kinetic model could be applied to describe adsorption mechanism of AR14 and BV3 dyes adsorption onto raw or modified clay materials. The classification of experimental adsorption isotherms of both dyes on AL−PILC showed a *S*−class isotherm, characteristic of multilayer adsorption due to the strong adsorbate-adsorbate interaction.

References

[1] B. Lellis, C. Z. F.-Polonio, J. A. Pamphile, J. C. Polonio, (2019). "Effects of textile dyes on health and the environment and bioremediation potential of living organisms," Biotechnology Research and Innovation, in press.

[2] X. Rong, F. Qiu, C. Zhang, L. Fu, Y. Wang, D. Yan, (2015), "Adsorption–photodegradation synergetic removal of methylene blue from aqueous solution by NiO/graphene oxide nanocomposite", Powder Technology, in press.

[3] H. B. Mansour, O. Boughzala, D. Dridi, D. Barillier, L. Chekir-Ghedira, R. Mosrati, (2011), " Les colorants textiles sources de contamination de l'eau: CRIBLAGE de la toxicité et des méthodes de traitement", Journal of Water Science, vol. 24, n° 3, 209-238.

[4] J. Chen, Y. Xiong, M. Duan, X. Li, Jun Li, S. Fang, S. Qin, R. Zhang, (2020), "Insight into the Synergistic Effect of Adsorption−Photocatalysis for the Removal of Organic Dye Pollutants by Cr-Doped ZnO", Langmuir, 35, 520-530.

[5] K. Chinoune, K. Bentaleb, Z. Bouberka, A. Nadim, U. Maschke, (2016), "Adsorption of reactive dyes from aqueous solution by dirty bentonite," Applied Clay Science, 123: 64–75.

[6] C. R. Sílvia Santos, A. R. Rui Boaventura, (2016), "Adsorption of cationic and anionic azo dyes on sepiolite clay: Equilibrium and kinetic studies in batch mode, Journal of Environmental Chemical Engineering, 4: 1473–1483.

[7] F. Güzel, H. Saygili, G. A Saygili, F. Koyuncu, (2014), "Elimination of anionic dye by using nanoporous carbon prepared from an industrial biowaste", Journal of Molecular Liquid, 194: 130–140.

[8] A. S. Abdulhameed, A. H. Jawad, A.-T. Mohammad, (2019), "Synthesis of chitosan-ethylene glycol diglycidyl ether/TiO_2 nanoparticles for adsorption of reactive orange 16 dye using a response surface methodology approach", Bioresource Technology 293: 122071.

[9] V. Sharma, P. Rekha, P. Mohanty, (2016), " Nanoporous hypercrosslinked polyaniline: An efficient adsorbent for the adsorptive removal of cationic and anionic dyes", Journal of Molecular Liquids 222: 1091–1100.

[10] M. H. Dehghani, M. Mohammadi, G. Mckay, (2016), "Equilibrium and Kinetic studies of of Trihalomethanes Adsorption onto Multiwalled Carbon Nanotubes", Water, Air, & Soil Pollution, 227: 332.

[11] T. S. Anirudhan and M. Ramachandran, (2015), " Adsorptive removal of basic dyes from aqueous solutions by surfactant modified bentonite clay (organoclay): Kinetic and competitive adsorption isotherm", Process Safety and Environmental Protection, 9 5: 215–225.

[12] R. Gottipati, S. Mishra, (2016), "Preparation of microporous activated carbon from Aegle Marmelos fruit shell and its application in removal of chromium (VI) from aqeous phase", Journal of Industrial and Engineering Chemistry, 36: 355−363.

[13] A. Ariful, I. Tariqul, C. I. Hernandez, M. L. Curry, (2018), "Adsorptive Ramoval of Sulfamethoxazole and Bisphenol A from contaminated Water using Functionalized Carbonaceous Material Derived from Tea Leaves", Journal of Environmental Chemical Engineering, 6 (4).

[14] B. Makhoukhi, M. Djab, M. A. Didi, (2015), "Adsorption of Telon dyes onto bis-imidazolium modified bentonite in aqueous solutions", Journal of Environmental Chemical Engineering, 3: 1384–1392.

[15] Li Wang and A. Wang, (2008), "Adsorption properties of Congo Red from aqueous solution onto surfactant-modified montmorillonite", Journal of Hazardous Materials 160 (2008) 173–180.

[16] M. Harouna, R. Djakba, J. P. Nguetnkam, B. B. Loura, D. N Ileana., J. M. Ketcha, (2015), "Adsorption of Mn^{2+} and Zn^{2+} in Aqueous Solution by Using Aluminum Pillared Clay from Boboyo (Far North Cameroon)", American Chemical Science Journal, 5 (1): 94−104.

[17] C. Tcheka, R. P. Chicinas, A. Maicaneanu, P. N. Fotsing, H. Moussout, R Domga, (2018), "Tetra-n-butylammonium Bromide (TBAB) Modified Cameroonian Local Clay Material for Adsorption of Crystal Violet Dye from Aqueous Solution", Submitted to Advancements in Materials, 2: 1-16.

[18] S. Yamanaka, G. W. Brindley, (1979), "High surface area solids obtained by reaction of montmorillonite with zirconyl chloride", Clays and Clay Minerals, Vol. 27, No. 2: 119-124.

[19] I. Khedher, A. Ghorbel, J. A. Mayoral, J. M. Fraile, "Physicochemical characterization of vanadium-doped alumina-pillared montmorillonite catalyst: Epoxidation of trans-2-hexen-1-ol", C. R. Chimie 12: 787−792.

[20] L. G. Yan, L. L. Qin, H. Q. Yu, S. Li, R. R. Shan, B. Du, (2015), "Adsorption of acid dyes from aqueous solution by CTMAB modified bentonite: Kinetic and isotherm modeling", Journal of Molecular Liquids 211: 1074–1081.

[21] H. Sadki, K. Ziat, M. Saidi, (2014), "Adsorption of dyes on activated local clay in aqueous solution", Journal of Materials and Environmental Science, 5: 2060−2065.

[22] F. Zermane, M. Baudu, (2015), "Influence of humic acids on the adsorption of Basic Yellow 28 dye onto an iron organo-inorgano pillared clay and two Hydrous Ferric Oxides", Journal of Industrial and Ingineering Chemistry, 25: 229−238.

[23] M. K. Dahri, M. R. Rahimi Kooh, B. L. Linda Lim, (2014), " Water remediation using low cost adsorbent walnut shell for removal of malachite green: Equilibrium, kinetics, thermodynamic and regeneration studies" Journal of Environmental Chemical Engineering 2: 1434–1444.

[24] L. C. Cotet, A. Maicaneanu, (2013), "AlphA-Cypermetrin Pesticide Adsorption on Carbon Aerogel Aerogel and Xerogel." Sci. Technol. 37–41.

[25] P. N. Fotsing, E. D. Woumfo, S. A. Maicaneanu, J. Vieillard, C. Tcheka, P. T. Ngueagni, Jean M. Siéwé, (2020), " Removal of Cu(II) from aqueous solution using a composite made from cocoa cortex and sodium alginate", Environmental Science and Pollution Research, https://doi.org/10.1007/s11356-019-07206-3.

[26] R. Elmoubarki, F. Z. Mahjoubi, H. Tounsadi, J. Moustadraf, M. Abdennouri, A. Zouhri,, A. El Albani, N. Barka, (2015), " Adsorption of textile dyes on raw and decanted Moroccan clays: Kinetics, equilibrium and thermodynamics", Water Resources and Industry, 9: 16–29

[27] S. Arellano-Cárdenas, S. López-Cortez, M. Cornejo-Mazón, J. C. Mares-Gutiérrez, (2013), "Study of malachite green adsorption by organically modified clay using a batch method", Applied Surface Science, 280: 74–78.

[28] A. A. Adeyemo, I. O. Adeoye, O. S. Bello, (2015), "Adsorption of dyes using different types of clay: a review", Appl Water Sci (2017) 7: 543–568.

[29] S. A. Yahya, M. I. El-Barghouthi, A. H. El-Sheikh, G. M. Walker, (2007), "Effect of Solution pH, Ionic Strength, and Temperature on Adsorption Behavior of Reactive Dyes on Activated Carbon", Dyes and pigments, p. 8.

[30] S. Lagergren, (1898), Kungliga Svenska Vetenskapsakad Handl, 24: 1–39.

[31] Y. S. HO and G. MCKAY, (1998), "Kinetic Models for the Sorption of Dye from Aqueous Solution by Wood", Trans IChemE, Vol 76, Part B.

[32] C. Xia, Y. Jing, Y. Jia, D Yue, J. Ma, X. Yin, (2011), " Adsorption properties of Congo Red from aqueous solution on modified hectorite: Kinetic and thermodynamic studies", Desalination 265: 81–87.

[33] J. W. J. Weber, J. C. Morris, (1963), J Sanit Eng Div Proceed Am Soc Civil Eng, 89: 31–59.

[34] W. H. Cheung, Y. S. Szeto, G. McKay, (2007), Bioresour. Technol., 98: 2897–2904.

[35] C H. Giles, D. Smith, (1974), "A General Treatment and Classification of the Solute Adsorption Isotherm I. Theoretical", Journal of Colloid and Interface Science, Vol. 47, No. 3.

[36] A. Djelad, A. Mokhtar, A Khelifa, A. Bengueddach, M. Sassi, (2019), "Alginate-whey an effective and green adsorbent for crystal violet removal: Kinetic, thermodynamic and mechanism studies", International Journal of Biological Macromolecules, in press.

[37] I. Langmuir *J Am Chem Soc*, 38 (1916). 2221-2295.

[38] Bike M., Etude Physico-Chimique de la Décoloration du Beurre de Karité et de l'Huile de Palme par le Charbon Actif de Coques de Noix de Pamiste et Trois Facteurs de Vertissol, Thèse de Doctorat Ecole Nationale Supérieur d'Agroindustrie, Université de Ngaoundéré, (2010) 237p.

[39] J. S. Piccin, L. Dotto, L. A. A. Pinto, (2011), " Adsorption Isotherms and Thermochemical Data of Fd&C Red N° 40 Binding by Chitosan", Brazilian Journal of Chemical Engineering, Vol. 28, No. 02, pp. 295-304.

[40] Saoud G., "Etude de la Carbonisation d'un Précursseur Végétal, les Noyaux d'Olive: Utilisation dans le Traitement des Eaux", Mémoire de Master, Université Skikida Algérie, (2008) 195p.

[41] M. Kessoum, O. C. Caqueret, B. Cagnon, S. Bostyn,, "Etude Cinétique et Thermodynamique de l'Adsorption des Composés Phénoliques en mono Soluté et Mélange de Charbon Actif", Journal of Water, vol. 3, (2008) p66-p72.

[42] N. T. Hai, Y. Sheng-Jie, H. Ahmad, C. Huan-Ping, (2017), "Mistakes and Inconsistencies Regarding Adsorption of Aontaminants from Aqueous Solution: A Critical Review", Wather Research, 10-17.

[43] Bouanimba N., "Modélisation et Optimisation de la Cinétique de Degradation Photocatalytique de Polluants Organiques en Solution Aqueuse", (2009), Mémoire de Master en Chimie, Faculté des Sciences, Université Mentouri- Constantine, 195p.